March 2018

Numerical investigation of 2D Vortex Induced and Wake Induced Vibrations of two circular cylinders in tandem arrangement

Simone MARTINI [a,1], Riccardo PIGAZZINI [a], Thomas PUZZER [a], Mitja MORGUT [a], Giorgio CONTENTO [a].

[a] *Dept. of Engineering and Architecture - University of Trieste, Italy*

Abstract. In ocean and offshore engineering, Vortex and Wake Induced Vibrations (VIV and WIV respectively) are serious issues related to the design and operational safety of offshore installations/structures.

VIV occur when vortices shed by a blunt freely-moving structure in steady (or unsteady) flow induce an oscillatory force on the structure, mostly in the direction perpendicular to the ambient flow. WIV take place when the oscillatory wake shed on the leeside of a structures hits a secondary element of the structure, inducing an oscillatory force on the latter.

VIV of a single elastically-mounted 2D cylinder has already been investigated by the authors and here used as reference case.

In this work, the crossflow motion of two elastically-mounted 2D cylinders in tandem arrangement is investigated via computationally efficient CFD URANS-based simulations. Two relevant cases are presented, the first one in which the upwind cylinder is fixed and the downwind cylinder is free to move and the second one where both are free to move.

Considering the strong complexity of the phenomena involved in VIV and WIV, considering also the relatively low computational effort (2D-RANS) adopted in this first step investigation, the results are in good agreement with experimental data, allowing a close insight in the coupling between wake and cylinder motion and providing a robust base for future more sophisticated simulations.

Keywords. Wake Induced Vibrations, Vortex Induced Vibrations, 2D URANS

1. Introduction

Flow Induced Motions (FIM) driven by vortex shedding are found in many marine engineering applications. Among others, catenary risers look particularly vulnerable to large displacements. Such umbilical structures are flexible and their cross sections are basically circular. Vortex shedding is therefore a very common feature of the induced down-

[1]Corresponding Author: Simone Martini, Dept. of Engineering and Architecture - University of Trieste, Italy; E-mail: simone.martini@phd.units.it, phone: +39-040-5582955.

stream flow and the related fluctuating pressure field on their surface may lead to VIV .

VIV response of marine risers may be further complicated by the presence of neighbor risers or tendons. When a riser is in the wake of an upstream blunt structure, the motion of the riser can be heavily altered and sometimes amplified. In this case, the motions experienced by the downstream structure are indicated as Wake Induced Vibrations (WIV).

In the quest of modelling the problem of VIV, Bokaian and Geoola[1] reported first results for rigid cylinders having only one degree of freedom. They performed experiments with two rigid cylinders in tandem, where the upstream cylinder was fixed while the downstream cylinder was free to move only transversally to the flow direction. They found that depending on the mass ratio, damping and spacing of the downstream cylinder "exhibited a vortex-resonance, or a galloping, or a combined vortex-resonance and galloping, or a separated vortex-resonance and galloping" response.

In a further study on the effect of mass and damping in this type of VIV, Zdravkovich and Medeiros[2] described new experiments where damping was varied systematically using electromagnets. The critical damping necessary to suppress VIV of the first cylinder and WIV of the second one was so determined.

Brika & Laneville[3] performed tests with a pair of long cylinders in a wind tunnel with a flexible cylinder positioned in the wake of a rigid cylinder at a distance ranging from 7 to 25 diameters. A series of curves for different separations reveal that as the separation increases, the interference effect of the upstream wake is reduced until the response resembles that of a single cylinder almost without any interference.

More recently, Assi et al. [4] performed experiments concerning flow-induced oscillations of circular cylinders in tandem arrangement placed in a water channel. A low mass ratio and low structural damping setup has been used and the predominance of the galloping-like phenomenon for the gap range from 3 to 6 diameters is clear. The peak amplitude observed for the downstream cylinder was about 50% higher than the one observed for the isolated cylinder case, confirming the strong presence of wake effects.

In this work, the crossflow motion of two elastically-mounted 2D cylinders in tandem arrangement is investigated via CFD URANS-based simulations. Two relevant cases are presented, the first one in which the upwind cylinder is fixed and the downwind cylinder is free to move and the second one where both are free to move. The paper is organized as follows: the benchmark case is described first; the computational framework is outlined; finally the results obtained are presented with discussion.

2. Benchmark case

Two circular cylinder (tandem arrangement) in uniform incident flow are mounted on two independent linear springs that allow them to move in cross flow direction only. The experimental work presented by Assi et al. [4] is here used as reference. It provides the full set of system proprieties, here used in the numerical study. Table 1 summarizes the main data. The uniform incident flow velocity is U, M is the cylinder mass, D the diameter, H is the structural damping, L the length of the cylinder and S is the distance between axes of the cylinders (in-lined with the incident flow).

A wide range of flow regimes, characterized by reduced velocity $U^* = U/(f_0 D)$, is taken into consideration. f_0 is the natural frequency of the system in fluid at rest. The

reduced velocity $U*$ is varied between 2 and 12 approximately, corresponding to sub-critical Reynolds numbers in the range $2.2 \cdot 10^3$ to $1.7 \cdot 10^4$. The mass/damping data used in the experiments and in the present simulations are such that the problem is characterized by low mass ratio $m^* = 1.92$ and low damping $\zeta = H/H_{cr} = 0.0068$ ratios. The study is performed using fresh water with the fluid density and the kinematic viscosity set to $\rho = 999.1026\,\mathrm{kg/m^3}$ and $\nu = 1.1386\,\mathrm{m^2\,s^{-1}}$ respectively.

Diameter of the cylinder	$D\,(\mathrm{mm})$	32
Spacing ratio	$S/D\,(-)$	5.0
Mass ratio	$m^* = \frac{M}{\rho \pi D^2 L/4}$	1.92
Damping Ratio	$\zeta\,(-)$	0.0068
Mass-damping parameter	$m^*\,\zeta\,(-)$	0.013
Natural frequency in water	$f_0\,(\mathrm{Hz})$	0.98

Table 1. Experimental/Numerical system proprieties

The value of the stiffness K used in the experiments was found from the undamped natural frequency in water, as given in [4]

$$f_0 = \frac{1}{2\pi}\sqrt{\frac{K}{M+M_A}} \tag{1}$$

M_A is the added mass, that can be rewritten as $M_A = C_A \cdot \rho \pi D^2 L/4$. C_A is the added mass coefficient. As a first approximation (potential flow), $C_A \approx 1.0$.

The structural damping H was obtained via the damping ratio ζ, as given in [4]. In the experiments [4], the damping coefficient was found from free decay tests in air, thus the following equation holds

$$H = \zeta\, 2\sqrt{K \cdot M}. \tag{2}$$

CFD simulations of free decay were run in order to check the assumptions used to derive K and H. From free decay decay tests in water, it turned out that the natural frequency was slightly underestimated by the simulations and thus the corresponding added mass coefficient had to be moved to $C_A \approx 1.1$. According to the latter, updated values of K and H were derived from eqs.1,2 and a new set of free decay simulations were run, showing a closer agreement with the experimental data. The updated mechanical properties were kept constant throughout the VIV and WIV simulations.

3. Computational setup

The numerical simulations were performed using the OpenFOAM library (release 2.4), an open source finite volume based CFD toolbox. The URANS approach was used and the workhorse Shear Stress Transport (SST) transport turbulence model was employed in order to close the system of the governing equations.

The openFOAM solver used for the simulation is `pimpleDyMFoam`, suitable for transient, incompressible flows involving dynamic meshes. For the PIMPLE loop, two corrector iterations and no non-orthogonal corrections were set. For time integration, first

order Euler implicit method was applied. Linear (CDS) and linearupwind (SOUDS) spatial discretization schemes were set for gradient and divergence terms, respectively. Preconditioned conjugate gradient (PCG) with diagonal incomplete Cholesky (DIC) was used to solve linear systems for pressure term with tolerance of 10^{-6}, preconditioned biconjugate gradient (PBiCG) with diagonal incomplete LU (DILU) were used for the pressure term linear system instead, setting the tolerance to 10^{-7}. For turbulence modeling, the $k-\omega-SST$ model was chosen. For k and ω smooth solver with Gauss-Siedel smoother was adopted.

Time domain simulations were carried out using the a first order implicit Euler scheme. The linear upwind scheme was used for the discretization of the advective terms. The linear limited (2nd order scheme) was used for the advective terms. The following boundary conditions were applied: on solid surfaces the no-slip condition was set. On Outlet boundary, a fixed valued of static pressure was imposed and on the side faces the symmetry condition was imposed. On the Inlet boundary, the free-stream velocity value was set, according to the different flow regimes investigated in this study.

3.1. Domain size and mesh generation

The shape of the computational domain used in the current simulations, with relevant dimensions, is sketched in figure 1. The characteristics of the mesh used in the present study obey the same principles adopted by the authors in a previous study on VIV of a single cylinder [5]. The mesh was generated using `snappyHexMesh`, a tool of the OpenFOAM library. The octree-based mesh shows refined layer at the cylinders' wall (with $y^+ < 1$) and a refinement region that surrounds both cylinders simultaneously. This solution (see figure 1b and 2) was preferred to the adoption of two separate refinement boxes because of the large run-time deformations encountered by the dynamic meshing in the narrow region between the two refinement boxes. An additional refinement box was added in order to resolve the wake field properly.

4. Results and comparison

The present CFD results are compared with experimental data from the literature, namely those presented by Assi et al. [4]. In figures 3 and 4 the non-dimensional amplitude of the motion of the cylinder $A^* = A/D$ and the non-dimensional dominant frequency of the motion $f^* = f/f_0$ are shown as functions of the reduced velocity $U^* = U/(D\,f_0)$. The cylinder's motion amplitude is evaluated using the mean value of the 10% of the highest peaks, according to [4].

4.1. VIV of single cylinder

The first case considered is the isolated single cylinder, free to oscillate in cross-flow direction (VIV). The mechanical restraints are the same used for the twin cylinder configuration and listed in table 1. A^* and f^* Vs U^* are shown in figure 3(a) and (b) respectively. The entire approach and resolution is the same adopted by the authors in another study [5]. In that investigation, the quality of the reproduction of experimental data from [6] was largely higher, still missing the right most part of the upper branch. In the literature, this is a well-known issue, related to the use of URANS simulations.

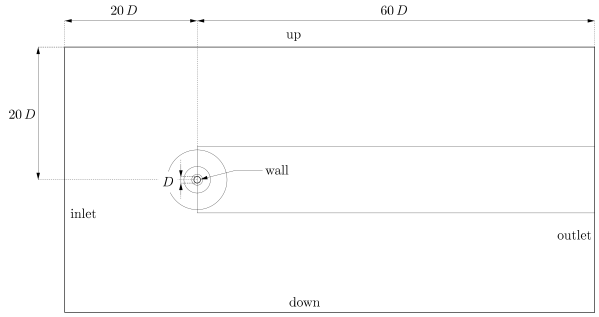

(a) Single cylinder

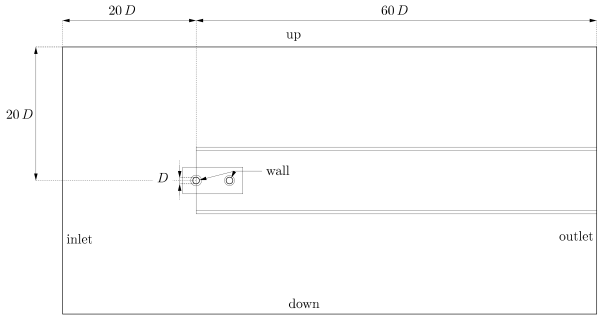

(b) Tandem configuration

Figure 1. Outline of the domain and refinement boxes.

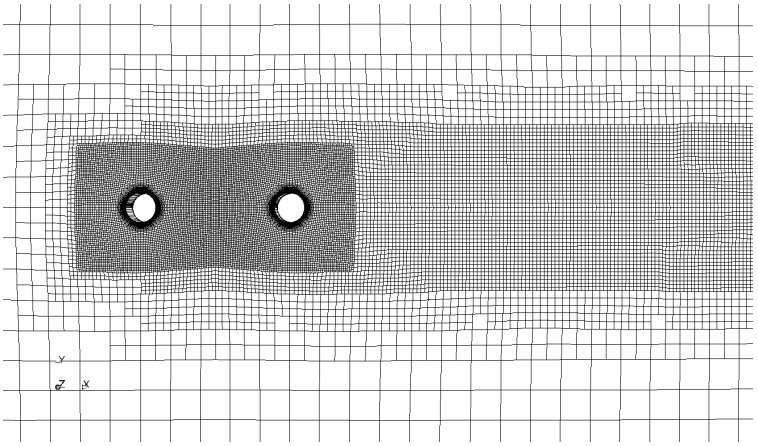

Figure 2. Mesh detail for two cylinders in tandem arrangement.

In the present study, the upper branch amplitudes could not be correctly reproduced both in terms of amplitudes and frequency. The initial and lower branches however shows a rather good agreement with experimental results, especially concerning the non-dimensional frequency response. Frequencies belonging to the lower branch follow the

Strouhal frequency (oblique dashed line). The anomaly in A^* for $U^* \approx 3.5$ can be related to the fact that f^* jumped abruptly to $f^* = 1$ (to be investigated further). In the lower branch, f^* follows the experimental values at $f^* \approx 1.3$ and amplitudes are closer to the experimental ones. A^* at the highest U^* values do not ketch the desinchronization regime, despite the excellent behavior of f^*.

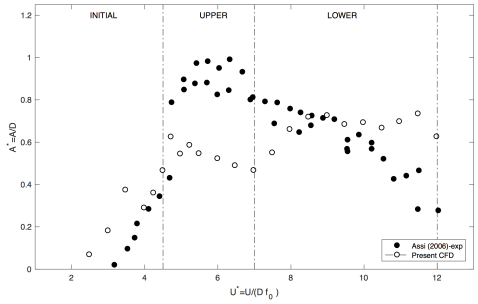

(a)

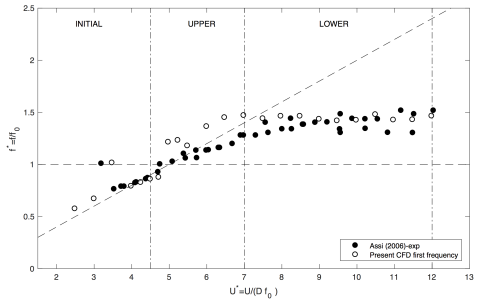

(b)

Figure 3. $A^* = A/D$ (a) and $f^* = f/f_0$ (b) Vs $U^* = U/(D\,f_0)$. Comparison between experimental data by Assi [4] (•) and present CFD results (○) for isolated single cylinder. The oblique dashed line in (c) corresponds to the Strouhal frequency (nominal Strouhal number=0.20).

4.2. VIV/WIV of downstream cylinder with fixed upwind cylinder

The characteristics of the response of a cylinder, freely moving in the crossflow direction and subject to the wake of a fixed upwind cylinder, are now analyzed. In this case, the motion of the downwind cylinder is characterized by both VIV and WIV, with predominance of the latter. Fig. 4a,c show the results, specifically A^* and f^* Vs U^*.

A^* exhibits a monotonic behavior, with a rapid growth at low U^*. The largest values are reached in the upper part of the range of U^*. The numerical simulations are in reasonable agreement with the experimental data, with a slight overestimate for low U^* (initial branch - $U^* \approx 2-5$) and a more pronounced underestimate for intermediate U^* (upper branch - $U^* \approx 5-7$).

f^* slightly overestimates the experimental data up to $U^* \approx 6$, still the overall behavior is very well reproduced.

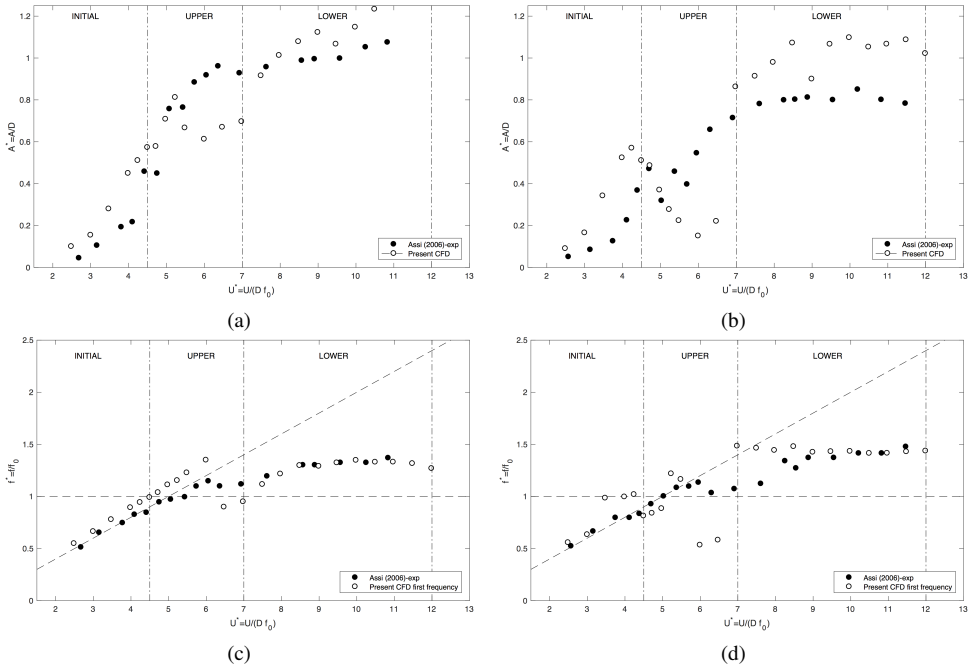

Figure 4. $A^* = A/D$ (a-b) and $f^* = f/f_0$ (c-d) Vs $U^* = U/(D\,f_0)$. Comparison between experimental data by Assi [4] (•) and present CFD results (○). The oblique dashed line in (c-d) corresponds to the Strouhal frequency (nominal Strouhal number=0.20).

4.3. VIV/WIV of downstream cylinder with freely moving upwind cylinder

The characteristics of the response of a cylinder, freely moving in the crossflow direction and subject to the wake of a freely moving upwind cylinder, are now analyzed. The wake released by the upstream cylinder is dominated by VIV. The latter, combined with WIV of the downstream cylinder, makes the problem rather complex, in terms of flow pattern and related motion response. Fig. 4b,d show the results, specifically A^* and f^* Vs U^*.

Experimental and numerical data show that A^* is no longer strictly monotonic (Fig. 4b Vs Fig. 4a), with a small drop in the lock-in region ($U^* \approx 5-7$), much more pronounced in the simulations. In the upper part of the range of U^* tested, A^* increases and reaches approximately 1, with a kind of saturation (see Fig. 4b).

Numerical values of A^* are only qualitatively comparable to the experimental one. Still, the main aspects of the motion are captured. Throughout the whole speed range, the same issues observed previously are found, namely overestimation of the amplitude in the initial and lower branch and underestimation in the upper branch. From the frequency response point of view, the initial branch is well represented only in the first part where the Strouhal frequency dominates. From $U^* \approx 3.5$ to 4.25 the natural frequency dominates the motion, resulting in large overestimation of the amplitude. Entering the upper branch the first three frequency ratio values suddenly drop near the Strouhal value, and the related amplitudes are significantly less overestimated. In the rest of the upper branch, frequencies are overestimated at first and then underestimated. The lower branch shows a significant jump in frequency response that gradually follows the experimental

values until $U^* \approx 11.5$. In this case too, the motion frequency in the lower branch shows better agreement with the experiments.

5. Conclusions

The flow around two cylinders in tandem arrangement was investigated by means of CFD simulations. Attention was focused on the cylinders flow induced motions due to vortex shedding. Three different cases were tested and the results compared to experimental data from the literature [4], ranging from an isolated moving single cylinder to fully moving twin cylinders.

As a general comment, the biggest differences between CFD and experimental data are always present in the lock-in/upper branch. Still, it can be observed that, despite the strong model limitations (modest discretisation, imposed two-dimensional flow and turbulence model), the main WIV motion characteristics have been captured.

Future development of the present work will be aimed at improving overall accuracy, and exploring the lock-in region by means of a 3D URANS/SAS approach. The benchmark case differs from the simulations mainly due to some flow three-dimensionality and free surface effects. A 3D approach using actual cylinder span and adequate spanwise resolution should result in a less coherent vortex structure and consequently effect on the motion forcing term, such as lower peak amplitudes and broader spectrum [6].

Acknowledgements

The Regional Program *POR FESR 2014 2020 - 1.3.b - Ricerca e sviluppo - Aree tecnologie marittime e smart health* of Regione Friuli-Venezia Giulia is acknowledged for providing the financial support of the SOPHYA Project.

The Scholarship co-funded by the EUROPEAN SOCIAL FUND, Axis 3 EDUCATION AND TRAINING, OPERATION ESF S3: Scholarships in FRIULI VENEZIA GIULIA is also acknowledged.

References

[1] A. Bokaian and F. Geoola, "Wake-induced galloping of two interfering circular cylinders," *Journal of Fluid Mechanics*, vol. 146, no. 1, pp. 383–415, 1984.

[2] M. Zdravkovich and E. Medeiros, "Effect of damping on interference-induced oscillations of two identical circular cylinders," *Journal of Wind Engineering and Industrial Aerodynamics*, vol. 38, no. 2-3, pp. 197–211, 1991.

[3] D. Brika and A. Laneville, "The flow interaction between a stationary cylinder and a downstream flexible cylinder," *Journal of Fluids and Structures*, vol. 13, no. 5, pp. 579–606, 1999.

[4] G. Assi, J. Meneghini, J. Aranha, P. Bearman, and E. Casaprima, "Experimental investigation of flow-induced vibration interference between two circular cylinders," *Journal of Fluids and Structures*, vol. 22, no. 6, pp. 819–827, 2006.

[5] R. Pigazzini, G. Contento, S. Martini, T. Puzzer, M. Morgut, and A. Mola, "Viv analysis of a single elastically-mounted 2d cylinder: Parameter identification of a single-degree-of-freedom multi-frequency model," *Journal of Fluids and Structures*, vol. 78, pp. 299 – 313, 2018.

[6] A. Khalak and C. Williamson, "Dynamics of a hydroelastic cylinder with very low mass and damping", *Journal of Fluids and Structures*, vol. 10, pp. 455 – 472, 1996.